Eigen-vibrations of Plates made of Functionally Graded Material

Holm Altenbach, Victor Eremeyev

Eigen-vibrations of Plates made of Functionally Graded Material

H. Altenbach[1] **and V. A. Eremeyev**[2]

Abstract: Within the framework of the direct approach to the plate theory we consider natural oscillations of plates made of functionally graded materials taking into account both the rotatory inertia and the transverse shear stiffness. It is shown that in some cases the results based on the direct approach differ significantly from the classical estimates. The reason for this is the non-classical computation of the transverse shear stiffness.

Keywords: functionally graded materials, foams, plate theories, direct approach, natural frequencies, rotatory inertia, effective stiffness, transverse shear stiffness

1 Introduction

Functionally graded materials (FGM) are composite materials where the composition or the microstructure are locally varied so that a certain variation of the local material properties is achieved. A nitrided steel, for instance, can be regarded as a FGM since on the microlevel a strong inhomogeneous structure can be observed. Modern FGMs are designed for complex requirements, such as the heat shield of a rocket or implants for humans. The gradual transition between the heat or corrosion resistant outer layer (often made of a ceramic material) and the tough metallic base material increases in most cases the life time of the component.

Another example of a FGM is a porous material with nonhomogeneous distribution of porosity (see Fig. 1).

Engineering structures made of porous materials, especially metal and polymer foams, have different applications last decades [Ashby, Evans, Fleck, Gibson, Hutchinson, and Wadley (2000); Banhart (2000); Gibson and Ashby (1997); Degischer and Kriszt (2002); Banhart, Ashby, and Fleck (1999); Landrock (1995); Lee and Ramesh (2004); Mills (2007)]. A metal or polymer foam is a cellular structure con-

[1] Martin-Luther-Universität Halle-Wittenberg, Germany.
[2] SSC of RASci and SFedU, Rostov on Don, Russia.

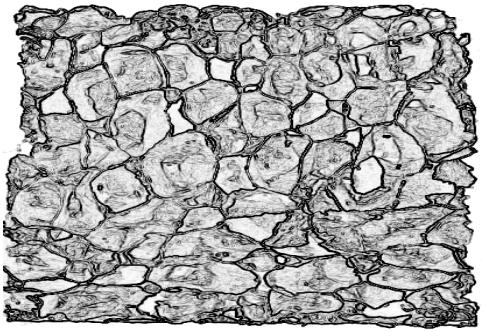

Figure 1: Nonhomogeneous structure of the metal foam

sisting of a solid metal or polymer, for example aluminium, steel, copper, polyurethane, etc., and containing a large volume fraction of gas-filled pores.

There are two types of foams. One is the closed-cell foam, while the second one is the open-cell foam. The defining characteristics of foams is the very high porosity: typically well over 80%, 90% and even 98% of the volume consists of void spaces. Another example of a perspective material is syntactic foam. This is a composite material synthesized by filling a metal, polymer or ceramic matrix with hollow particles called microballoons (see, e.g., Gupta and Ricci (2006); El Hadek and Tippur (2003)). Functionally graded plates and shells are considered by Allahverdizadeh, Naei, and Bahrami (2008); Arciniega and Reddy (2007); Batra (2007); Wu and Liu (2007); Chen and Tan (2007); Efraim and Eisenberger (2007); He, Ng, Sivashanker, and Liew (2001); Matsunaga (2004); Nie and Zhong (2007); Praveen and Reddy (1998); Reddy (2000); Roque, Ferreira, and Jorge (2007) among others. They present different theories based on hypotheses or mathematical treatments of the three-dimensional equations.

The suggested theories can be classified mostly as

- first order shear deformation theories or
- higher order theories

The first one are based on the improvement of the strains introducing independent translations and rotations of the points of the mid-plane of the plate. The advantage of such theories is that the number of boundary conditions corresponds to the order of the governing equations. In addition, all variables have a clear physical interpretation. The disadvantage is related to the presentation of the transverse shear.

Constitutive equations can be established for the transverse shear but they do not reflect correctly the plate behavior. In most engineering approaches in this case, a transverse shear correction is introduced and one gets more or less satisfying results. But the definitions for the shear correction are not unique, and so we have many different suggestions in the literature (see, e.g., Altenbach (2000a,b)).

The second class of theories is very popular in the computational community. Starting with the pioneering contributions of Levinson (1980) and Reddy (1984), systematically new theories were established. In the authors' opinion, these theories are free from the necessity to introduce a shear correction. But it is easy to check that they have several disadvantages too. At first, the interpretation of the higher-order terms is not clear, in general. At second, not in any case the boundary conditions on the lower and the upper faces are fulfilled. Last, but not least, not all theories are consistent in the sense of Kienzler (2002).

Here we present another approach which is free of assumptions about the three-dimensional stress and deformation states. Instead of the shear correction or higher order terms an alternative method of estimation the transverse shear stiffness is applied. On the other hand, the identification of elastic constants in the two-dimensional constitutive equations is a non-trivial problem. It is shown in Altenbach and Zhilin (1988); Zhilin (1976, 2006) among others that the concept of effective properties can support the handling of the identification. The identification of the effective stiffness properties can be performed with the help of static two-dimensional and corresponding three-dimensional boundary value problems (tension superposed with bending, plane shear, and torsion) and the comparison of the forces and moments in the sense of averaged stresses or stress resultants. In Zhilin (2006) the same effective stiffness properties are obtained by comparison of the spectrum of natural frequencies of the three-dimensional rectangular plate-like body and the spectrum of the simply-supported 5-parametric rectangular plate with rotatory inertia. Let us note that in major two-dimensional theories of plates effects such as some boundary effects, through-the-thickness waves, etc., cannot be properly described and one needs to use the three-dimensional elasticity in this case. But the global static analysis and the determination of the low values of eigenfrequencies can be performed by using two-dimensional approaches.

2 Governing Equations of a Two-dimensional Plate Theory

The direct approach is based on the Cosserat theory in continuum mechanics. In continuum mechanics two different models can be introduced: the non-polar or the polar. The polar continuum is more natural for plates. In the first of a non-polar continuum case only force actions are assumed. From this it follows the symmetry of the stress tensor and only translations are considered. For the second model one

has force and moment actions. From this it follows that there are a symmetric and a nonsymmetric stress tensor and translations and rotations can be suggested independently. Now any continuum (three-, two- or one-dimensional) can be introduced in a natural way: geometrical relations (kinematics), material independent balances of mass, momentum, moment of momentum, energy, entropy and the material dependent equations (constitutive equations and evolution equations). Finally, one needs boundary and possibly initial conditions.

2.1 Symbolic Presentation of the Equations

Since the direct approach is the natural way to describe the behavior of plates (the stress resultants which are used in most of plate theories can be regarded as forces and moments) a two-dimensional plate theory which allows to model homogeneous and inhomogeneous plates can be presented as follows. The basics are presented in Altenbach and Zhilin (1988, 2004); Zhilin (1976).

2.1.1 Linear Basic Equations

Let us introduce the following assumption:

The plate (homogeneous or inhomogeneous in the transverse direction) can be represented by a deformable surface.

In addition, the theory presented here is limited to small displacements and rotations and the quadratic strain energy (for example, rubber-like materials cannot be analyzed by these equations). Each material point is an infinitesimal rigid body with 5 degrees of freedom (3 translations and 2 rotations). The following governing equations can be introduced:

- Fist and second Euler's law (balances of momentum and moment of momentum)

$$\begin{aligned} &\nabla \cdot T + q = \rho \ddot{\boldsymbol{u}} + \rho \boldsymbol{\Theta}_1 \cdot \ddot{\boldsymbol{\varphi}}, \\ &\nabla \cdot \boldsymbol{M} + \boldsymbol{T}_\times + \boldsymbol{m} = \rho \boldsymbol{\Theta}_1^{\mathrm{T}} \cdot \ddot{\boldsymbol{u}} + \rho \boldsymbol{\Theta}_2 \cdot \ddot{\boldsymbol{\varphi}}. \end{aligned} \tag{1}$$

  Here $\boldsymbol{T}$, $\boldsymbol{M}$ are the tensors of forces and moments, $\boldsymbol{q}$, $\boldsymbol{m}$ are the vectors of surface loads (forces and moments), $T_\times$ is the vector invariant of the force tensor [Lurie (2005)], $\boldsymbol{\nabla}$ is the nabla (Hamilton) operator (pseudovector), $u, \boldsymbol{\varphi}$ are the vectors of the displacements and the rotations, $\Theta_1, \boldsymbol{\Theta}_2$ are the first and the second tensor of inertia, ρ is the density (effective property of the deformable surface), $(\ldots)^{\mathrm{T}}$ denotes the transposed tensor and $\dot{(\ldots)}$ the time derivative.

- Geometrical relations

$$\begin{aligned} &\boldsymbol{\mu} = (\nabla \boldsymbol{u} \cdot \boldsymbol{a})^{\mathrm{sym}}, \\ &\gamma = \nabla \boldsymbol{u} \cdot n + c \cdot \varphi, \\ &\boldsymbol{\kappa} = \nabla \boldsymbol{\varphi}. \end{aligned} \tag{2}$$

a is the first metric tensor, n is the unit normal vector, $\boldsymbol{c} = -\boldsymbol{a} \times \boldsymbol{n}$ is the discriminant tensor [Zhilin (2006)], $\boldsymbol{\mu}$, $\boldsymbol{\gamma}$ and $\boldsymbol{\kappa}$ are the strain tensors (tensor of in-plane strains, vector of transverse shear strains and tensor of the out-of-plane strains), $(\ldots)^{\mathrm{sym}}$ denotes symmetric part of the tensor.

- Boundary conditions

$$\begin{aligned} &\nu \cdot \boldsymbol{T} = f, \quad \nu \cdot \boldsymbol{M} = l \quad (l \cdot \boldsymbol{n} = 0) \quad \text{or} \\ &u = u^0, \quad \varphi = \boldsymbol{\varphi}^0 \quad \text{along } S. \end{aligned} \tag{3}$$

Here $\boldsymbol{f}$ and l are external force and couple vectors acting along the boundary of plate S, while $\boldsymbol{u}^0$ and $\boldsymbol{\varphi}^0$ are given functions describing the displacements and rotation of the plate boundary, respectively. $\boldsymbol{\nu}$ is the unit normal vector to S ($\boldsymbol{\nu} \cdot \boldsymbol{n} = 0$). The relations (3) are the static and the kinematic boundary conditions. Other types of boundary conditions are possible. For example, the boundary conditions corresponding to a hinge are given by

$$\nu \cdot \boldsymbol{M} \cdot \tau = 0, \quad u = \boldsymbol{0}, \quad \varphi \cdot \tau = 0. \tag{4}$$

τ is the unit tangent vector to S ($\tau \cdot n = \boldsymbol{\tau} \cdot \boldsymbol{\nu} = 0$).

2.1.2 Two-dimensional Constitutive Equations

Limiting our discussion to the elastic behavior, the following statements for the constitutive modeling can be done. At first, the strain energy can be expanded in a Taylor series limited to quadratic terms. In addition, we assume that the eigenstresses can be neglected (the linear terms in the series are dropped out).

- The general representation of the strain energy of the deformable surface W is given by

$$\begin{aligned} W(\boldsymbol{\mu}, \gamma, \boldsymbol{\kappa}) = \quad & \frac{1}{2} \boldsymbol{\mu} \cdot\cdot A \cdot\cdot \mu + \mu \cdot\cdot B \cdot\cdot \kappa \\ & + \frac{1}{2} \kappa \cdot\cdot C \cdot\cdot \kappa + \frac{1}{2} \gamma \cdot \Gamma \cdot \boldsymbol{\gamma} \\ & + \gamma \cdot (\boldsymbol{\Gamma}_1 \cdot\cdot \boldsymbol{\mu} + \boldsymbol{\Gamma}_2 \cdot\cdot \kappa). \end{aligned} \tag{5}$$

$A, B, \boldsymbol{C}$ are 4th rank tensors, $\boldsymbol{\Gamma}_1, \Gamma_2$ are 3rd rank tensors, Γ is a 2nd rank tensor of the effective stiffness properties. They depend on the material properties and the thickness geometry. In the general case the tensors contain 36

different values - a reduction is possible assuming some symmetries. $\cdot\cdot$ is the double dot product.

- From Eq. (5) the following constitutive equations may be derived
  - the in-plane forces

$$T \cdot \boldsymbol{a} = \frac{\partial W}{\partial \boldsymbol{\mu}} = \boldsymbol{A} \cdot\cdot \boldsymbol{\mu} + \boldsymbol{B} \cdot\cdot \kappa + \boldsymbol{\gamma} \cdot \boldsymbol{\Gamma}_1. \tag{6}$$

  - the transverse forces

$$\boldsymbol{T} \cdot \boldsymbol{n} = \frac{\partial W}{\partial \boldsymbol{\gamma}} = \boldsymbol{\Gamma} \cdot \boldsymbol{\gamma} + \boldsymbol{\Gamma}_1 \cdot\cdot \boldsymbol{\mu} + \boldsymbol{\Gamma}_2 \cdot\cdot \boldsymbol{\kappa}. \tag{7}$$

  - the moments

$$M^{\mathrm{T}} = \frac{\partial W}{\partial \boldsymbol{\kappa}} = \mu \cdot\cdot B + C \cdot\cdot \boldsymbol{\kappa} + \boldsymbol{\gamma} \cdot \Gamma_2. \tag{8}$$

Let us consider the through-the-thickness symmetric structure of the plate and isotropic material behavior. In this case instead of the general form of the effective stiffness tensors one gets [Zhilin (2006)]

$$\begin{array}{lcl} \boldsymbol{A} & = & A_{11} a_1 a_1 + A_{22}(\boldsymbol{a}_2 \boldsymbol{a}_2 + a_4 a_4), \\ C & = & C_{22}(a_2 a_2 + a_4 a_4) + C_{33} a_3 \boldsymbol{a}_3, \\ \boldsymbol{\Gamma} & = & \Gamma a, \qquad \boldsymbol{B} = \boldsymbol{0}, \\ \boldsymbol{\Gamma}_1 & = & \boldsymbol{0}, \qquad \Gamma_2 = 0 \end{array}$$

with

$$\begin{array}{ll} \boldsymbol{a}_1 = \boldsymbol{a} = \boldsymbol{e}_1 \boldsymbol{e}_1 + \boldsymbol{e}_2 \boldsymbol{e}_2, & \boldsymbol{a}_2 = \boldsymbol{e}_1 \boldsymbol{e}_1 - \boldsymbol{e}_2 \boldsymbol{e}_2, \\ \boldsymbol{a}_3 = c = e_1 \boldsymbol{e}_2 - \boldsymbol{e}_2 \boldsymbol{e}_1, & \boldsymbol{a}_4 = e_1 e_2 + e_2 e_1. \end{array}$$

$e_1, \boldsymbol{e}_2$ are unit basic vectors. In addition, one obtains the orthogonality condition for the $\boldsymbol{a}_i$ $(i = 1,2,3,4)$

$$\frac{1}{2} \boldsymbol{a}_i \cdot\cdot a_j = \delta_{ij}, \qquad \delta_{ij} = \begin{cases} 1, & i = j, \\ 0, & i \neq j \end{cases}.$$

Further we consider two cases:

Case 1: Homogeneous plates – all properties are constant (no dependency of the thickness coordinate z).

Case 2: Inhomogeneous plates (sandwich, multilayered, functionally graded) – all properties are functions of z.

In the case of inhomogeneous, but isotropic behavior the material properties are described by parameters depending on z

$$E = E(z), \qquad \nu = \nu(z),$$
$$G = G(z) = \frac{E(z)}{2(1+\nu(z))}, \quad \rho_0 = \rho_0(z).$$

E is the Young's modulus, ν is the Poisson's ratio, G is shear modulus, while ρ_0 is the density.

The identification of the stiffness tensors is proved by Zhilin (2006); Altenbach (2000a,b). The following results are established:

- the in-plane stiffness tensor components

$$A_{11} = \frac{1}{2}\left\langle \frac{E}{1-\nu} \right\rangle,$$
$$A_{22} = \frac{1}{2}\left\langle \frac{E}{1+\nu} \right\rangle = < G >, \tag{9}$$

- the plate stiffness tensor components

$$C_{33} = \frac{1}{2}\left\langle \frac{E}{1-\nu} z^2 \right\rangle,$$
$$C_{22} = \frac{1}{2}\left\langle \frac{E}{1+\nu} z^2 \right\rangle = < Gz^2 >, \tag{10}$$

- the transverse shear stiffness tensor component

$$\Gamma = \lambda^2 C_{22} \tag{11}$$

with λ following from

$$\frac{\mathrm{d}}{\mathrm{d}z}\left(G\frac{\mathrm{d}Z}{\mathrm{d}z}\right) + \lambda^2 GZ = 0, \quad \left.\frac{\mathrm{d}Z}{\mathrm{d}z}\right|_{|z|=\frac{h}{2}} = 0, \tag{12}$$

see Altenbach and Zhilin (1988); Zhilin (2006), and $< (\ldots) >$ is the integral over the thickness h.

The tensors of inertia and the plate density are given in Altenbach and Zhilin (1988); Zhilin (2006)

$$\begin{aligned} &\rho = \langle \rho_0 \rangle, \quad \rho\Theta_1 = -\langle \rho_0 z \rangle c, \\ &\rho\boldsymbol{\Theta}_2 = \Theta\boldsymbol{a}, \quad \Theta = \langle \rho_0 z^2 \rangle. \end{aligned} \tag{13}$$

The assumed symmetry with respect of the plate mid-plane results in $\Theta_1 = \mathbf{0}$. Θ characterizes the rotatory inertia of the plate cross section.

2.2 Basic Equations for Isotropic Plates in Cartesian Coordinates

Let us assume the Cartesian coordinate system x_1, x_2 (in-plane coordinates) and z (orthogonal to the mid-plane). Then the unit normal vectors are $\boldsymbol{e}_1, \boldsymbol{e}_2$ and n. With respect to the introduced coordinate system the following representations are valid:

- Displacement and rotation vectors

$$u = u_1 e_1 + u_2 \boldsymbol{e}_2 + w\boldsymbol{n}, \quad \varphi = -\varphi_2 \boldsymbol{e}_1 + \varphi_1 \boldsymbol{e}_2. \tag{14}$$

  $u_\alpha (\alpha = 1,2)$ are the in-plane displacements, w is the deflection and φ_α are the rotations about the axes $\boldsymbol{e}_\alpha$, respectively.

- Force and moment tensors

$$\begin{aligned} \boldsymbol{T} &= T_1 \boldsymbol{e}_1 \boldsymbol{e}_1 + T_{12}(\boldsymbol{e}_1 \boldsymbol{e}_2 + \boldsymbol{e}_2 \boldsymbol{e}_1) \\ &\quad + T_2 e_2 \boldsymbol{e}_2 + T_{1n} e_1 \boldsymbol{n} + T_{2n} e_2 \boldsymbol{n}, \\ \boldsymbol{M} &= M_1 \boldsymbol{e}_1 \boldsymbol{e}_2 - M_{12}(\boldsymbol{e}_1 \boldsymbol{e}_1 - \boldsymbol{e}_2 \boldsymbol{e}_2) \\ &\quad - M_2 \boldsymbol{e}_2 e_1. \end{aligned} \tag{15}$$

  T_α, T_{12} are the in-plane forces, $T_{\alpha n}$ are the transverse shear forces, M_α are the bending moments and M_{12} is the torsion moment.

- Strain tensors

$$\begin{aligned} \boldsymbol{\mu} &= \mu_1 e_1 e_1 + \mu_{12}(\boldsymbol{e}_1 \boldsymbol{e}_2 + \boldsymbol{e}_2 e_1) + \mu_2 e_2 e_2, \\ \boldsymbol{\gamma} &= \gamma_1 \boldsymbol{e}_1 + \gamma_2 \boldsymbol{e}_2, \\ \kappa &= \kappa_1 \boldsymbol{e}_1 \boldsymbol{e}_2 - \kappa_{12} e_1 \boldsymbol{e}_1 + \kappa_{21} \boldsymbol{e}_2 e_2 - \kappa_2 e_2 \boldsymbol{e}_1. \end{aligned}$$

  μ_α are the strains, μ_{12} is the shear strain, γ_α are the transverse shear strains, κ_α are the bending deformations and κ_{12} is the torsion deformation.

- External loads

$$q = q_1 e_1 + q_2 \boldsymbol{e}_2 + q_n \boldsymbol{n}, \quad m = -m_2 e_1 + m_1 e_2. \tag{16}$$

  q_α are the in-plane loads, q_n is the transverse load, m_α are the moments.

Now the first and the second Euler's law, the geometrical relations and the constitutive equations take the form:

- First and second Euler's law

$$\begin{aligned} T_{1,1}+T_{12,2}+q_1 &= \rho\ddot{u}_1, \\ T_{12,1}+T_{2,2}+q_2 &= \rho\ddot{u}_1, \\ T_{1n,1}+T_{2n,2}+q_n &= \rho\ddot{w}, \\ M_{1,1}+M_{12,2}-T_{1n}+m_1 &= \Theta\ddot{\varphi}_1, \\ M_{12,1}+M_{2,2}-T_{2n}+m_2 &= \Theta\ddot{\varphi}_2. \end{aligned} \tag{17}$$

- Boundary conditions (for brevity, S is a part of line $x_1 = \text{const}$ ($\boldsymbol{\nu} = e_1$, $\boldsymbol{\tau} = \boldsymbol{e}_2$), and we present here only simple support boundary conditions)

$$M_1 = 0, \;\; u_1 = u_2 = w = 0, \;\; \varphi_2 = 0. \tag{18}$$

- Geometrical relations

$$\begin{aligned} \mu_1 &= u_{1,1}, & \mu_2 &= u_{2,2}, \\ \mu_{12} &= \frac{1}{2}(u_{1,2}+u_{2,1}), & & \\ \gamma_1 &= w_{,1}+\varphi_1, & & \\ \gamma_2 &= w_{,2}+\varphi_2, & & \\ \kappa_1 &= \varphi_{1,1}, & \kappa_2 &= \varphi_{2,2}, \\ \kappa_{12} &= \varphi_{2,1}, & \kappa_{21} &= \varphi_{1,2}. \end{aligned} \tag{19}$$

- Constitutive equations

$$\begin{aligned} T_1 &= (A_{11}+A_{22})\mu_1+(A_{11}-A_{22})\mu_2, \\ T_2 &= (A_{11}-A_{22})\mu_1+(A_{11}+A_{22})\mu_2, \\ T_{12} &= 2A_{22}\mu_{12}, \\ T_{1n} &= \Gamma\gamma_1, \quad T_{2n} = \Gamma\gamma_2, \\ M_1 &= (C_{33}+C_{22})\kappa_1+(C_{33}-C_{22})\kappa_2, \\ M_2 &= (C_{33}-C_{22})\kappa_1+(C_{33}+C_{44})\kappa_2, \\ M_{12} &= C_{22}(\kappa_{12}+\kappa_{21}). \end{aligned} \tag{20}$$

From the last equations can be seen that the A_{ij} are the effective in-plane stiffness tensor components, the C_{ij} are the effective plate stiffness tensor components, and Γ is the transverse shear stiffness.

3 Examples of Effective Stiffness and Inertia

3.1 Homogeneous Plate

The simplest test for the correctness of the estimated stiffness properties is the homogeneous isotropic plate. In this case the density and the rotatory inertia coefficient are

$$\rho = \rho_0 h, \quad \Theta = \frac{\rho_0 h^3}{12}. \tag{21}$$

The classical plate (bending) stiffness follows as

$$C_{33} + C_{22} = \frac{Eh^3}{12(1-\nu^2)} \tag{22}$$

and can be found in textbooks, e.g. Timoshenko and Woinowsky-Krieger (1985). The transverse shear stiffness follows from (11). Finally one obtains

$$\Gamma = \frac{\pi^2}{h^2}\frac{Gh^3}{12} = \frac{\pi^2}{12}Gh. \tag{23}$$

$\pi^2/12$ is a factor which is similar to the shear correction factor which was first introduced by Timoshenko (1921) in the theory of beams. Here this factor is a result of the non-classical establishment of the transverse shear stiffness. Comparing this value with the Mindlin's estimate $\pi^2/12$ [Mindlin (1951)] and the Reissner's estimate $5/6$ [Reissner (1944)] one concludes that the direct approach yields the same value as Mindlin's theory (note that Mindlin's shear correction is based on the solution of a dynamic problem, here is used the solution of a static problem[1]). Reissner's value differs slightly.

3.2 Classical Sandwich Plate in Reissner's Sense

Now we assume the following geometry: h_c is the core thickness and h_f the thickness of the face sheets ($h_c \gg h_f$). The material properties of the core and the face sheets are E_c, E_f, G_c, G_f, ρ_{c0}, ρ_{f0} with $E_c \ll E_f$, $G_c \ll G_f$, $\rho_{c0} \ll \rho_{f0}$. With the

[1] It must be underlined that the result (23) is independent of whether a static or a dynamic problem is investigated. This is shown in Zhilin (1976).

thickness $h = h_c + h_f$ one gets

$$A_{11} = \frac{1}{2}\left(\frac{E_f h_f}{1-\nu_f} + \frac{E_c h_c}{1-\nu_c}\right),$$
$$A_{22} = \frac{1}{2}\left(\frac{E_f h_f}{1+\nu_f} + \frac{E_c h_c}{1+\nu_c}\right),$$
$$C_{33} = \frac{1}{24}\left[\frac{E_f (h^3 - h_c^3)}{1-\nu_f} + \frac{E_c h_c^3}{1-\nu_c}\right],$$
$$C_{22} = \frac{1}{24}\left[\frac{E_f (h^3 - h_c^3)}{1+\nu_f} + \frac{E_c h_c^3}{1+\nu_c}\right].$$

The density and the rotatory inertia coefficient are

$$\rho = \rho_{c0} h_c + \rho_{f0} h_f, \quad \Theta = \frac{\rho_{c0} h_c^3}{12} + \frac{\rho_{f0}(h^3 - h_c^3)}{12}. \tag{24}$$

The bending stiffness results in

$$C_{33} + C_{22} = \frac{1}{12}\left[\frac{E_f (h^3 - h_c^3)}{1-\nu_f^2} + \frac{E_c h_c^3}{1-\nu_c^2}\right].$$

The transverse shear stiffness can be computed from the following transcendent equation [Altenbach (2000a)]

$$\mu \cos\gamma(1-\alpha)\cos\gamma\alpha - \sin\gamma(1-\alpha)\sin\gamma\alpha = 0$$

with

$$\gamma = \lambda\frac{h}{2}, \quad \alpha = \frac{h_c}{h}, \quad \mu = \frac{G_c}{G_f}$$

μ and α take the values $0 \le \mu < \infty$ and $0 \le \alpha \le 1$. A typical sandwich structure has a very weak core and thin face sheets. Then the bending stiffness and the transverse shear stiffness can be approximated by

$$C_{33} + C_{22} = \frac{1}{4}\frac{E_f h^2 h_f}{1-\nu_f^2}, \qquad \Gamma = G_c h. \tag{25}$$

This solutions was first obtained by Reissner (1947).

3.3 Functionally Graded Material

In this section we consider small deformations of a functionally graded plate made of metallic or polymeric foams. For the panel made from porous metallic foams the distribution of the pores over the thickness can be inhomogeneous. Let us introduce h as the thickness of the panel, ρ_s as the density of the bulk material and ρ_p as the minimum value of the density of the foam. For the description of the symmetric distribution of the porosity we assume the power law

$$V(z) = \alpha + (1-\alpha)\left|\frac{2z}{h}\right|^n, \tag{26}$$

where $\alpha = \rho_p/\rho_s$, n is the power. $n = 0$ corresponds to the homogeneous plate, for $n = 1$ we have the linear distribution of the porosity through the thickness. The distribution can be established, for example, if the plate is made of two symmetric layers. If $n > 1$ one has a more complex distribution. If $n \gg 1$ the plate core has an approximately constant porosity, but the distribution of the density in the face layers is significant inhomogeneous. Examples of the distribution are shown in Fig. 2 for $n = 0, 1, 10, 50$ with $\alpha = 0.1$.

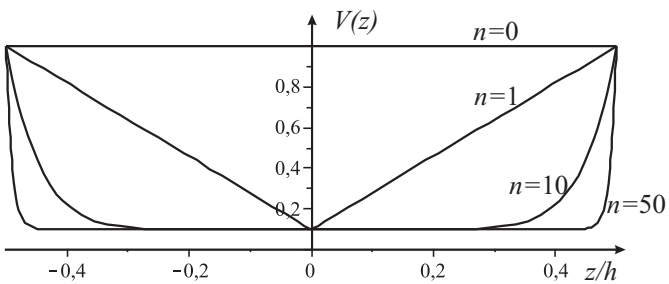

Figure 2: Distribution of porosity

The elastic properties of a metallic foam highly depend on the porosity and the cell structure. The dependence of the Young's modulus and the shear modulus on the porosity is given by the power law [Ashby, Evans, Fleck, Gibson, Hutchinson, and Wadley (2000); Gibson and Ashby (1997)]

$$\frac{E_p}{E_s} \sim \alpha^m, \qquad \frac{G_p}{G_s} \sim \alpha^m, \tag{27}$$

where E_p and G_p are the Young modulus and the shear modulus of the foam, respectively, E_s and G_s are the Young modulus and the shear modulus of the material

which is used to synthesize the foam. The value m depends on the structure of the foam. For the closed-cell foams $m = 1$, for the open-cell foams $m \approx 2$. Based on experimental data presented in Ashby, Evans, Fleck, Gibson, Hutchinson, and Wadley (2000); Gibson and Ashby (1997) one can assume $\nu = \text{const}$. Finally, we obtain that $A_{11}, A_{22}, C_{33}, C_{22}$ are related by

$$A_{11} = \frac{1+\nu}{1-\nu} A_{22}, \qquad C_{33} = \frac{1+\nu}{1-\nu} C_{22}. \tag{28}$$

For $m = 2$ (open cell foam) A_{22} and C_{22} are given by

$$\begin{aligned} A_{22} &= G_{\mathrm{s}} h \left[\alpha^2 + \frac{2\alpha(1-\alpha)}{n+1} + \frac{(1-\alpha)^2}{2n+1} \right], \\ C_{22} &= \frac{G_{\mathrm{s}} h^3}{12} \left[\alpha^2 + \frac{6\alpha(1-\alpha)}{n+3} + \frac{3(1-\alpha)^2}{2n+3} \right]. \end{aligned} \tag{29}$$

For $m = 1$ (closed cell foam)

$$\begin{aligned} A_{22} &= G_{\mathrm{s}} h \left[\alpha + \frac{1-\alpha}{n+1} \right], \\ C_{22} &= \frac{G_{\mathrm{s}} h^3}{12} \left[\alpha + \frac{3(1-\alpha)}{n+3} \right]. \end{aligned} \tag{30}$$

For $n \gg 1$ one can conclude that in both cases (29) and (30) tend to the following approximations $A_{22} \approx G_{\mathrm{p}} h$ and $C_{22} \approx G_{\mathrm{p}} h^3/12$, but for finite values of n the values of $A_{11}, A_{22}, C_{33}, C_{22}$ depend on the relation between α and n. Let us introduce the notation for the effective bending stiffness as it follows

$$D_{\mathrm{eff}} = C_{33} + C_{22}.$$

The values of the normalized D_{eff} versus n is given in Fig. 3.

Here $\alpha = 0.1$, D_{K} is defined by the formula $D_{\mathrm{K}} = E_{\mathrm{s}}/[12(1-\nu^2)]$ which is analogous to Eq. (22) with $E = E_{\mathrm{s}}$, and the dashed lines correspond to the effective bending stiffness calculated by Reissner's formulae (25). One can see that Reissner's approach gives lower bounds for the effective bending stiffness of a FGM plate. To obtain the dependence of the transverse shear stiffness one has to solve Eq. (12). The solution of the spectral problem (12) is found numerically by using the shooting method [Stoer and Bulirsch (1980)]. The values of normalized Γ versus n is given in Fig. 4. Here we have $m = 2$, $\alpha = 0.1$, $\nu = 0.3$.

The density and the rotatory inertia coefficient are

$$\begin{aligned} \frac{1}{\rho_{\mathrm{s}}} \rho &= \alpha h + \frac{(1-\alpha) h}{n+1}, \\ \frac{1}{\rho_{\mathrm{s}}} \Theta &= \frac{1}{12} \alpha h^3 + \frac{1}{4} \frac{(1-\alpha) h^3}{3+n}. \end{aligned} \tag{31}$$

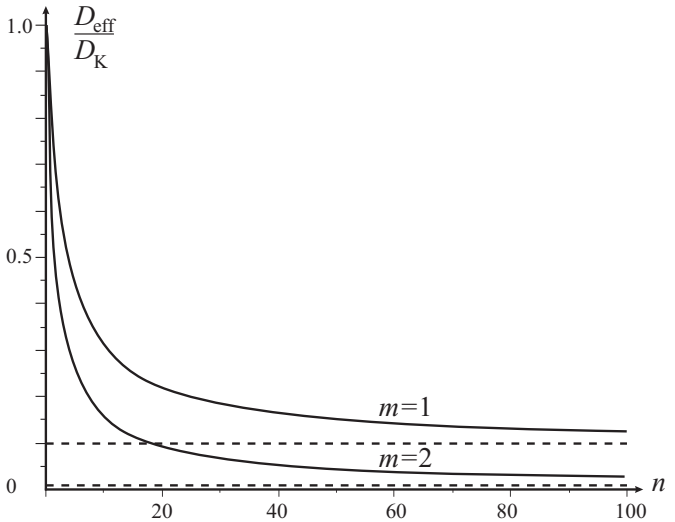

Figure 3: Normalized effective bending stiffness vs. n

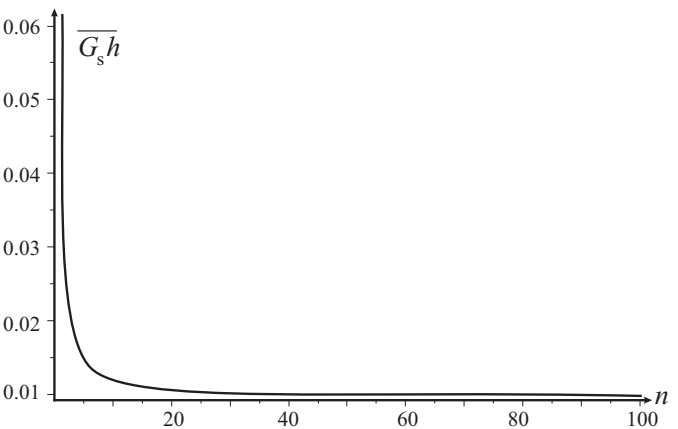

Figure 4: Normalized transverse shear stiffness vs. n

From (31) one can see that for $n \gg 1$ one obtains $\rho \approx \rho_{\mathrm{p}} h$ and $\Theta \approx \rho_{\mathrm{p}} h^3/12$ which are coincide with (24) if $h_{\mathrm{f}} \to 0$.

4 Equations of Motion for a Symmetric Isotropic Plate

In this case Eqs (17) split into two parts: plane problem for the tangential displacements u_1 and u_2, and the bending problem for the w, φ_1 and φ_2, respectively. In Cartesian coordinates with the geometrical relations (19) Eqs $(17)_{1,2}$ reduce to the form

$$\begin{aligned} &(A_{11}+A_{22})u_{1,11}+(A_{11}-A_{22})u_{2,21} \\ &\qquad +A_{22}(u_{1,21}+u_{2,11})+q_1 \;=\; \rho\ddot{u}_1, \\ &(A_{11}-A_{22})u_{1,12}+(A_{11}+A_{22})u_{2,22} \\ &\qquad +A_{22}(u_{1,22}+u_{2,12})+q_2 \;=\; \rho\ddot{u}_2. \end{aligned} \tag{32}$$

The Eq. $(17)_3$ has the following form

$$\Gamma(w_{,11}+w_{,22})+\Gamma(\varphi_{1,1}+\varphi_{2,2})+q_n=\rho\ddot{w}. \tag{33}$$

The Eqs $(17)_{4,5}$ result in

$$\begin{aligned} &(C_{33}+C_{22})\varphi_{1,11}+(C_{33}-C_{22})\varphi_{2,21} \\ &+C_{22}(\varphi_{1,22}+\varphi_{2,12})-\Gamma\varphi_1-\Gamma w_{,1}+m_1=\Theta\ddot{\varphi}_1, \\ &(C_{33}+C_{22})\varphi_{2,22}+(C_{33}-C_{22})\varphi_{1,12} \\ &+C_{22}(\varphi_{1,21}+\varphi_{2,11})-\Gamma\varphi_2-\Gamma w_{,2}+m_2=\Theta\ddot{\varphi}_2. \end{aligned} \tag{34}$$

To eliminate the functions φ_1 and φ_2 from Eqs (33) and (34) let us differentiate the first equation of (34) with respect to x_1, while the second one with respect to x_2. Summing up these equations one gets

$$\begin{aligned} &[(C_{33}+C_{22})\Delta-\Gamma](\varphi_{1,1}+\varphi_{2,2})-\Gamma\Delta w \\ &+m_{1,1}+m_{2,2}=\Theta(\ddot{\varphi}_{1,1}+\ddot{\varphi}_{2,2}). \end{aligned} \tag{35}$$

Here $\Delta(\ldots)=(\ldots)_{,11}+(\ldots)_{,22}$.

Using (33) we can eliminate $\varphi_{1,1}+\varphi_{2,2}$ from Eq. (35). Thus, we obtain one equation with respect to w

$$\begin{aligned} &(C_{33}+C_{22})\Delta\Delta w+\rho\ddot{w}+\frac{\rho\Theta}{\Gamma}w^{(4)} \\ &\quad-\left(\Theta+\rho\frac{C_{33}+C_{22}}{\Gamma}\right)\Delta\ddot{w} \\ &\quad=q_n+\frac{\Theta}{\Gamma}\ddot{q}_n-\frac{C_{33}+C_{22}}{\Gamma}\Delta q_n+m_{1,1}+m_{2,2}. \end{aligned} \tag{36}$$

Here $w^{(4)}=\dfrac{\partial^4 w}{\partial t^4}$.

5 Free oscillations and dispersion curves of a rectangular plate

To analyze the influence of the transverse shear stiffness and the rotatory inertia on the natural frequencies let us consider natural oscillations of a rectangular plate with simple-support type boundary conditions. Let us assume that $m_1 = m_2 = 0$, $q_n = 0$, $x_1 \in [0,a]$, $x_2 \in [0,b]$, where a and b are the length and the width of the plate. Thus, we can rewrite Eq. (36) in the following form

$$D_{\text{eff}}\Delta\Delta w + \rho\ddot{w} + \frac{\rho\Theta}{\Gamma}w^{(4)} - \left(\Theta + \rho\frac{D_{\text{eff}}}{\Gamma}\right)\Delta\ddot{w} = 0. \tag{37}$$

Introducing dimensionless variables by

$$\bar{w} = h^{-1}w, \quad \bar{x}_1 = h^{-1}x_1,\ \bar{x}_2 = h^{-1}x_2,$$
$$\bar{x}_1 \in \left[0, \frac{a}{h}\right],\ \bar{x}_2 \in \left[0, \frac{b}{h}\right], \quad \bar{t} = T^{-1}t,\ T^2 = \frac{\rho h^4}{D_{\text{eff}}},$$

Equation (37) transforms to

$$\Delta\Delta\bar{w} + \ddot{\bar{w}} + \beta\bar{w}^{(4)} - \zeta\Delta\ddot{\bar{w}} = 0. \tag{38}$$

Here

$$\Delta = \frac{\partial^2}{\partial\bar{x}_1^2} + \frac{\partial^2}{\partial\bar{x}_2^2},$$

while

$$\beta = \frac{\Theta D_{\text{eff}}}{\rho\Gamma h^4}, \qquad \zeta = \frac{1}{h^2}\left(\frac{\Theta}{\rho} + \frac{D_{\text{eff}}}{\Gamma}\right)$$

are dimensionless parameters.

Let us note that, if one considers the limiting case with $\Gamma \to \infty$ and $\Theta = 0$, then $\beta = \zeta = 0$. Thus, the equation of motion for the Kirchhoff plate follows immediately from Eq. (38) as

$$\Delta\Delta\bar{w} + \ddot{\bar{w}} = 0. \tag{39}$$

Obviously, Eq. (38) contains two small parameters β and ζ and can be considered as a singular perturbation of Eq. (39). While the small parameters are the coefficients of the derivatives with respect to time of higher order, than one can find the difference between the solutions of Eqs (38) and (39) for highly oscillated modes. Equation (38) contains a term with a small parameter on the mixed derivative with respect to time and space.

The solution of (38) can be given by

$$\bar{w} = W_{mn} \exp(i\omega\bar{t}) \sin\frac{\pi h m \bar{x}_1}{a} \sin\frac{\pi h n \bar{x}_2}{b}, \tag{40}$$

where m, $n = 1, 2\ldots$ are integer numbers, W_{mn} is the dimensionless magnitude of the oscillations.

The solution (40) describes the natural oscillations of the plate where ω and η are connected by the dispersion relation

$$\eta^4 - \omega^2 + \beta\omega^4 - \zeta\eta^2\omega^2 = 0, \tag{41}$$

where

$$\eta^2 = \left(\frac{\pi h m}{a}\right)^2 + \left(\frac{\pi h n}{b}\right)^2.$$

All natural frequencies of the plate have to satisfy the dispersion relation $\omega = \omega(\eta)$ which is the solutions of Eq. (41).

Let us consider the solutions of (41) for different approaches to the plate theory. For the Kirchhoff-plate theory we have $\Gamma \to \infty$, $\Theta = 0$. Then $\beta = \zeta = 0$ and one gets the standard dispersion relation

$$\omega = \eta^2. \tag{42}$$

Considering the Mindlin-plate theory without rotatory inertia ($\Theta = 0$) we can use Eqs (21) – (23). Then we obtain that $\beta = 0$ and $\zeta = 2/(1-\nu)$. For example, for $\nu = 1/3$ one gets $\beta = 3$. The dispersion relation is given by

$$\omega = \frac{\eta^2}{\sqrt{1+\zeta\eta^2}}. \tag{43}$$

The dispersion curve given by Eq. (43) coincides with the dispersion curve in the Kirchhoff-plate theory when $\eta \ll 1$, but for $\eta \gg 1$ coincides with the asymptotic line $\omega = \eta/\sqrt{\zeta}$. The dispersion curves are shown in Fig. 5. The solid curves marked by labels K and M correspond to Eqs (42) and (43), respectively. Here $\nu = 1/3$ is assumed.

For the Reissner's sandwich plate theory we use Eqs (25) and assume that $\Theta = 0$. Then again $\beta = 0$. Let us consider the sandwich plate core made of metal foam while the faces made of material used to synthesize the foam. Introducing the notations $E_\mathrm{f} = E_\mathrm{s}$, $G_\mathrm{c} = G_\mathrm{p}$, etc., and applying Eqs (27) with the assumption $\nu_\mathrm{c} = \nu_\mathrm{f} = \nu$ we obtain

$$\zeta = \frac{h_\mathrm{f}}{2h(1-\nu)\alpha^m}. \tag{44}$$

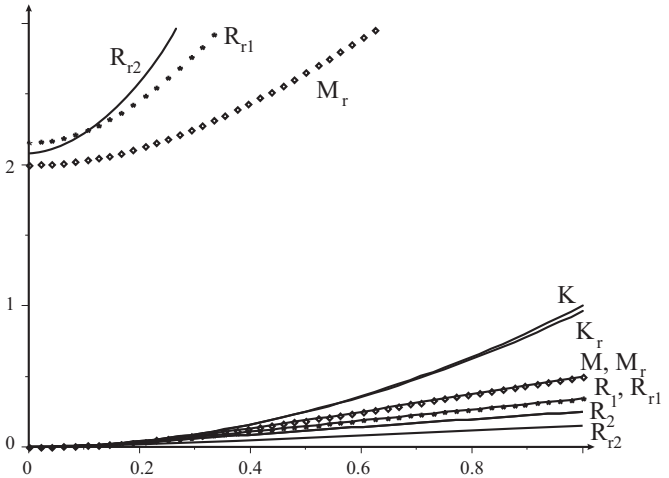

Figure 5: Dispersion curves: K – Kirchhoff plate; M – Mindlin plate; R_1 and R_2 – Reissner sandwich plates with $h_{\rm f} = 0.1h$, $\alpha = 0.1$, and $h_{\rm f} = 0.05h$, $\alpha = 0.05$, respectively. $\rm K_r$, $\rm M_r$, $\rm R_{r1}$, and $\rm R_{r2}$ are the corresponding dispersion curves with taking into account the rotatory inertia

For instance, if $h_{\rm f} = 0.1h$, $\alpha = 0.1$, $m = 2$, $\nu = 1/3$ then $\zeta = 7.5$. For $h_{\rm f} = 0.05h$, $\alpha = 0.05$, $m = 2$, $\nu = 1/3$ one gets $\zeta = 15$. The corresponding dispersion curves are shown in Fig. 5. They are marked by labels $\rm R_1$ and $\rm R_2$, respectively.

Let us investigate the influence of the rotatory inertia ($\Theta \neq 0$). For the Kirchhoff-type plate theory with $\Gamma \to \infty$ we obtain from Eq. (21) that $\beta = 0$ while $\zeta = 1/12$. Thus, we have the dispersion relation (43) with a fixed value of ζ. The corresponding dispersion curve is marked by the label $\rm K_r$ in Fig. 5. One can see that, if we neglect the transverse shear stiffness, then the influence of the rotatory inertia is not significant.

For the Mindlin-type plate theory we obtain that

$$\beta = \frac{1}{6(1-\nu)}, \quad \zeta = \frac{1}{12} + \frac{2}{1-\nu}.$$

Thus, in this case we have dispersion equations in the general form (41). For $\nu = 1/3$ the corresponding dispersion curve is marked by the label $\rm M_r$ in Fig. 5 using point style with box markers. One can see that for $\beta \neq 0$ the qualitative behavior of the dispersion curves is quite different. A new branch appears starting from the point $\eta = 0$, $\omega = 1/\sqrt{\beta}$.

In the case $\beta \neq 0$, Eq. (41) has two solutions given by

$$\omega_{\pm} = \left[\frac{1+\zeta\eta^2 \pm \sqrt{(1+\zeta\eta^2)^2 - 4\beta\eta^4}}{2\beta} \right]^{1/2}. \tag{45}$$

One solution of (45) starts from the point $(0,0)$ in the $\eta - \omega$ diagram, while the second one starts from the point $\left(0, 1/\sqrt{\beta}\right)$. Both curves have linear asymptotes when $\eta \to \infty$

$$\omega_{\pm} = \eta \left[\frac{\zeta \pm \sqrt{\zeta^2 - 4\beta}}{2\beta} \right]^{1/2}, \quad \eta \gg 1. \tag{46}$$

The solution ω_{-} describes the bending low-frequency oscillation modes or bending waves in the case of an infinite plate, while ω_{+} describes high-frequency oscillations.

For the sandwich plate with non-zero rotatory inertia we obtain that

$$\begin{aligned} \frac{\Theta}{h^2\rho} &= \frac{1}{12}\left[1 - \frac{h_{\mathrm{c}}^3}{h^3}(1-\alpha)\right]\left[1 - \frac{h_{\mathrm{c}}}{h}(1-\alpha)\right]^{-1}, \\ \frac{D_{\mathrm{eff}}}{h^2\Gamma} &= \frac{h_{\mathrm{f}}}{2h(1-\nu)\alpha^m}. \end{aligned} \tag{47}$$

The corresponding dispersion curves are shown in Fig. 5 for two sets of values $h_{\mathrm{f}} = 0.1h$, $\alpha = 0.1$, $m = 2$, $\nu = 1/3$ and $h_{\mathrm{f}} = 0.05h$, $\alpha = 0.05$, $m = 2$, $\nu = 1/3$. They are marked by the labels $\mathrm{R_{r1}}$ (point style with asterisk markers) and $\mathrm{R_{r2}}$ (solid line), respectively.

Note that for the chosen values of the material and geometrical parameters some of the curves are practically coincide with each other. Indeed, the low branch of the $\mathrm{M_r}$-curve coincides with the M-curve, while the low branch of the $\mathrm{R_{r1}}$-curve coincides with the $\mathrm{R_1}$-curve.

Let us discuss the FGM plates in detail. Using Eqs (31), (28), and (11) we obtain that

$$\begin{aligned} \frac{\Theta}{h^2\rho} &= \frac{1}{4}\left[\frac{1}{3}\alpha + \frac{1-\alpha}{3+n}\right]\left[\alpha + \frac{1-\alpha}{n+1}\right]^{-1}, \\ \frac{D_{\mathrm{eff}}}{h^2\Gamma} &= \frac{2}{1-\nu}\frac{1}{h^2\lambda^2}. \end{aligned}$$

Note that λ^2 is the minimal eigen-value of the Sturm-Liouville problem (12) [Altenbach (2000a,b)]. For the FGM plate it can be solved as in the previous case

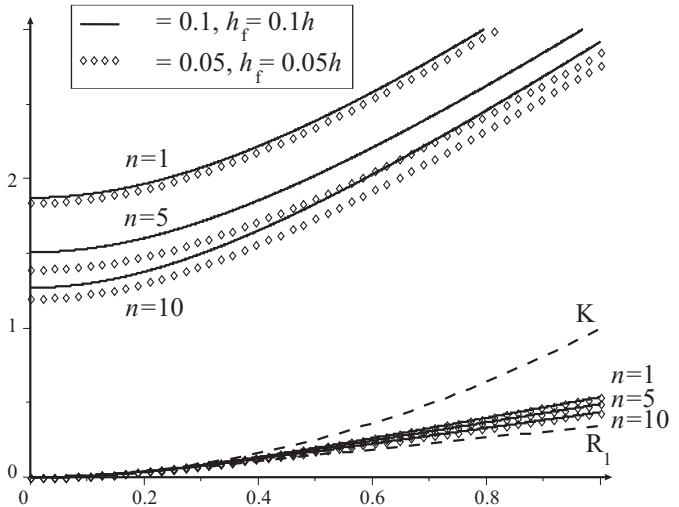

Figure 6: Dispersion curves for a FGM plate for two sets of material and geometrical parameters

applying the shooting method. In Fig. 6 we present the dispersion curves for different values of n and α with $m = 2$, $\nu = 0.3$. Dashed curves in Fig. 6 correspond to Kirchhoff's and Reissner's solutions, marked by labels K and R_1, respectively. One can see that the influence of α is significant in the case of the high-oscillating branches of the dispersion curves. For low-oscillating branch, the difference between the values $\alpha = 0.1$ and $\alpha = 0.05$ is very small. For the low dispersion curves, the Kirchhoff's and the Reissner's solutions can be used as the upper and the lower bounds of the eigen-frequencies of a FGM plate. One can see that the Reissner's sandwich-plate approach demonstrates a good qualitative coincidence with our results on a FGM plate as well as the Mindlin's one. On the other hand, the classical plate models cannot describe the high-oscillating solutions corresponding to our dispersion curves for ω_+.

The normalized first eigen-frequencies of a quadratic plate are presented in Table 1. Here $a = b$, $h = 0.1a$, $\nu = 0.3$, $m = 2$, $\Omega = \omega/\omega_K$, and ω_K is the first eigen-frequency of the Kirchhoff plate given by (42). One can see that for thick plates the structure of the plate has an influence on the eigen-frequencies. The Kirchhoff theory gives us larger values of the eigen-frequency, while Reissner's theory gives us smaller values of the eigen-frequency. So, they can be used as a estimation for the modal analysis of FGM plates.

Table 1: Minimal normalized eigen-frequency of a quadratic plate and corresponding values of the normalized transverse shear stiffness and the rotatory inertia

Model description	$\Gamma/G_{\mathrm{s}}h$	$\Theta/\rho h^2$	Ω
Kirchhoff's plate	∞	0	1
Mindlin's plate	$\pi^2/12$	0	0.799
Reissner's sandwich plate			
$\alpha = 0.1$, $h_{\mathrm{f}} = 0.1$	0.01	0	0.644
$\alpha = 0.05$, $h_{\mathrm{f}} = 0.05$	0.025	0	0.512
Kirchhoff-type plate	∞	1/12	0.992
Mindlin-type plate	$\pi^2/12$	1/12	0.797
Reissner-type sandwich plate			
$\alpha = 0.1$, $h_{\mathrm{f}} = 0.1$	0.01	0.028	0.644
$\alpha = 0.05$, $h_{\mathrm{f}} = 0.05$	0.025	0.015	0.511
FGM plate $\alpha = 0.1$ $n = 1$	0.061	0.12	0.818
$n = 5$	0.015	0.15	0.734
$n = 10$	0.012	0.14	0.782

The considered example demonstrates that the theory of sandwich plates may be not sufficient to describe the oscillations of FGM plates which are highly non-homogeneous in the thickness direction. The theory of laminated plates (see, e.g. Altenbach, Altenbach, and Kissing (2004)) may be more useful, but here the problem of the determination of the number of layers and its properties appears.

6 Summary and Outlook

In the paper Altenbach and Eremeyev (2008), we analyzed the influence of the transverse shear stiffness on the static behavior of FGM plates. Here we present the analysis of FGM plates in dynamics taking into account not only the transverse shear stiffness but the rotatory inertia as well. We have shown that both parameters play a significant role in dynamics. In particular, the non-zero rotatory inertia enables us to describe the high-oscillating solutions. We established the bounds for the natural frequencies of FGM plates. The presented approach to model FGM plates within the framework of a 5-parametric theory of plates has an advantage with respect to theories of sandwich or laminated plates which do not take into account the transverse shear stiffness and the rotatory inertia or based on a fixed shear correction since some results are more accurate, other results cannot be obtained

by the classical approach.

Acknowledgement: The research work was supported by DFG grant 436RUS17/-21/07, by the Martin-Luther-University Halle-Wittenberg and the program of development of the South Federal University (Rostov on Don, Russian Federation).

References

Allahverdizadeh, A.; Naei, M.; Bahrami, M. (2008): Nonlinear free and forced vibration analysis of thin circular functionally graded plates. *J. Sound Vibration*, vol. 310, pp. 966–984.

Altenbach, H. (2000): An alternative determination of transverse shear stiffnesses for sandwich and laminated plates. *Int. J. Solids Struct.*, vol. 37, no. 25, pp. 3503–3520.

Altenbach, H. (2000): On the determination of transverse shear stiffnesses of orthotropic plates. *ZAMP*, vol. 51, pp. 629–649.

Altenbach, H.; Altenbach, J.; Kissing, W. (2004): *Mechanics of composite structural elements*. Springer-Verlag, Berlin.

Altenbach, H.; Eremeyev, V. (2008): Direct approach based analysis of plates composed of functionally graded materials. *Archive of Applied Mechanics*, vol. 78, no. 10, pp. 775–794.

Altenbach, H.; Zhilin, P. (1988): A general theory of elastic simple shells (in Russ.). *Uspekhi Mekhaniki*, vol. 11, no. 4, pp. 107–148.

Altenbach, H.; Zhilin, P. A. (2004): The theory of simple elastic shells. In Kienzler, R.; Altenbach, H.; Ott, I.(Eds): *Critical review of the theories of plates and shells and new applications*, Lect. Notes Appl. Comp. Mech. 16, pp. 1–12. Springer, Berlin.

Arciniega, R.; Reddy, J. (2007): Large deformation analysis of functionally graded shells. *In. J. Solids Struct.*, vol. 44, no. 6, pp. 2036–2052.

Ashby, M. F.; Evans, A. G.; Fleck, N. A.; Gibson, L. J.; Hutchinson, J. W.; Wadley, H. N. G. (2000): *Metal foams: a design guid*. Butterworth-Heinemann, Boston.

Banhart, J. (2000): Manufacturing routes for metallic foams. *Journal of the Minerals*, vol. 52, no. 12, pp. 22–27.

Banhart, J.; Ashby, M. F.; Fleck, N. A.(Eds): *Metal foams and porous metal structures*. Verlag MIT Publishing, Bremen.

Batra, R. C. (2007): High-order shear and normal deformable theory for functionally graded incompessible linear elastic plates. *Thin-walled structures*, vol. 45, pp. 974–982.

Chen, C.-S.; Tan, A.-H. (2007): Imperfection sensitivity in the nonlinear vibration of initially stresses functionally graded plates. *Composite Structures*, vol. 78, pp. 529–536.

Degischer, H. P.; Kriszt, B.(Eds): *Handbook of cellular metals. Production, Processing, applications*. WILEY-VCH, Weinheim.

Efraim, E.; Eisenberger, M. (2007): Exact vibration analysis of variable thickness thick annular isotropic and fgm plates. *J. Sound Vibration*, vol. 299, pp. 720–738.

El Hadek, M. A.; Tippur, H. V. (2003): Dynamic fracture parameters and constraint effects in functionally graded syntactic epoxy foams. *Int. J. Solids Struct.*, vol. 40, pp. 1885–1906.

Gibson, L. J.; Ashby, M. F. (1997): *Cellular solids: structure and properties*. Cambridge Solid State Science Series. Cambridge University Press, Cambridge, 2nd edition.

Gupta, N.; Ricci, W. (2006): Comparison of compressive properties of layered syntactic foams having gradient in microballoon volume fraction and wall thickness. *Materials Science and Engng. A*, vol. 427, pp. 331–342.

He, X.; Ng, T.; Sivashanker, S.; Liew, K. (2001): Active control of FGM plates with integrated piezoelectric sensors and actuators. *Int. J. Solids Struct.*, vol. 38, pp. 1641 – 1655.

Kienzler, R. (2002): On consistent plate theories. *Arch. Appl. Mech.*, vol. 72, pp. 229 – 247.

Landrock, A. H.(Ed): *Handbook of plastic foams. types, properties, manufactore and applications*, Park Ridge, New Jersey, 1995. Noes Publications.

Lee, S.; Ramesh, N.(Eds): *Polymeric Foams. Mechanisms and Materials*, Boca Raton, 2004. CRC Press.

Levinson, M. (1980): An accurate, simple theory of the statics and dynamics of elastic plates. *Mech. Res. Comm.*, vol. 7, no. 6, pp. 343 – 350.

Lurie, A. I. (2005): *Theory of elasticity*. Foundations of Engineering Mechanics. Springer, Berlin.

Matsunaga, H. (2004): Free vibration and stability of laminated composite circular arches subjected to initial axial stress. *J. Sound Vibration*, vol. 271, pp. 651–670.

Mills, N. (2007): *Polymer foams handbook. Engineering and biomechanics applications and design guide*. Butterworth-Heinemann, Amsterdam.

Mindlin, R. D. (1951): Influence of rotatory inertia and shear on flexural motions of isotropic elastic plates. *Trans. ASME. J. Applied Mechanics*, vol. 18, pp. 31–38.

Nie, G.; Zhong, Z. (2007): Semi-analytical solution for three-dimensional vibration of functionally graded circular plates. *Methods Appl. Mech. Engng.*, vol. 196, pp. 4901–4910.

Praveen, G. N.; Reddy, J. N. (1998): Nonlinear transient thermoelastic analysis of functionally graded ceramic-metal plates. *Int. J. Solids Struct.*, vol. 35, pp. 4457–4476.

Reddy, J. N. (1984): A simple higher-order theory for laminated composite plates. *Trans . ASME. J. Appl. Mech.*, vol. 51, pp. 745 – 752.

Reddy, J. N. (2000): Analysis of functionally graded plates. *Int. J. Numer. Methods Engng.*, vol. 47, pp. 663–684.

Reissner, E. (1944): On the theory of bending of elastic plates. *J. Math. Phys.*, vol. 23, pp. 184–194.

Reissner, E. (1947): On bending of elastic plates. *Quart. Appl. Math.*, vol. 5, pp. 55–68.

Roque, C. M. C.; Ferreira, A. J. M.; Jorge, R. M. N. (2007): A radial basis function approach for the free vibration analysis of functionally graded plates using a refined theory. *J. Sound Vibration*, vol. 300, pp. 1048–1070.

Stoer, J.; Bulirsch, R. (1980): *Introduction to numerical analysis*. Springer, New York.

Timoshenko, S. P. (1921): On the correnction for shear of the differential equation for transverse vibrations of prismatic bars. *Phil. Mag. Ser. 6(245)*, vol. 41, pp. 744–746.

Timoshenko, S. P.; Woinowsky-Krieger, S. (1985): *Theory of plates and shells*. McGraw Hill, New York.

Wu, C.-P.; Liu, K.-Y. (2007): A State Space Approach for the Analysis of Doubly Curved Functionally Graded Elastic and Piezoelectric Shells. *CMC: Computers, Materials & Continua*, vol. 6, pp. 177 – 200.

Zhilin, P. A. (1976): Mechanics of deformable directed surfaces. *Int. J. Solids Struct.*, vol. 12, pp. 635 – 648.

Zhilin, P. A. (2006): *Applied mechanics. Foundations of the theory of shells (in Russ.)*. St. Petersburg State Polytechnical University.